Kernel-Based Identification of Non-Causal Systems with Application to Inverse Model Control ⋆

Lennart Blanken [a], Tom Oomen [a]

[a] *Eindhoven University of Technology, Department of Mechanical Engineering, Control Systems Technology Group, P.O. Box 513, 5600 MB Eindhoven, The Netherlands*

Abstract

Models of inverse systems are commonly encountered in control, e.g., feedforward. The aim of this paper is to address several aspects in identification of inverse models, including model order selection and dealing with unstable inverse systems that originate from inverting non-minimum phase dynamics. A kernel-based regularization framework is developed for identification of non-causal systems. It is shown that 'unstable' models can be viewed as bounded, but non-causal, operators. As the main contribution, a range of the required kernels for non-causal systems is developed, including non-causal stable spline kernels. Benefits of the approach are confirmed in an example, including non-causal feedforward control for non-minimum phase systems.

Key words: Kernel-based regularization; system identification; reproducing kernel Hilbert space; non-causal systems; feedforward control

1 Introduction

Identification of inverse models has recently attracted interest from the perspective of identification for feedforward control. Identification of models for feedback control has been well developed, see, e.g., [13,15]. The dual question of identification for feedforward control has recently led to the observation that it may pose advantages to directly identify the inverse model from data, see, e.g., [5,19], compared to identification of a forward model and subsequent model inversion.

Developments in identification for feedforward control are mainly directed towards the use of low-order parametric inverse models, with key focus on estimation procedures that lead to small variance of the estimated parameters. The use of low-order finite impulse response filters is investigated in [22], which is further extended in [5] towards an instrumental variable (IV) algorithm to deliver unbiased estimates with minimal variance. These techniques have been extended towards rational model structures, see, e.g., [1,31]. The model structure and order are often selected based on physical insight, i.e., grey-box, or in combination with regularization techniques to promote low-order models, see, e.g., [25].

Although identification of inverse models has been substantially developed from several perspectives, the essential issue of model order selection is not yet fully addressed, and is mostly done in an ad hoc manner. The aim of this paper is to address the issue of model order selection by revisiting the identification of inverse models in light of recent developments in system identification, in particular kernel-based regularization. Essentially, a different perspective on priors is taken, e.g., no longer fixing a discrete model order. A central aspect is that instability of inverse models is a direct result of non-minimum phase (NMP) dynamics of the system. The key step in this paper is that unstable models are viewed as non-causal and bounded operators, which is in sharp contrast to the common perspective of causal but unbounded operators. Indeed, non-causality is crucial to compensate NMP dynamics in feedforward control [32,33].

Kernel-based regularization techniques, see, e.g., [20,26,29], allow a different approach to specifying

⋆ This work is supported by Océ Technologies, P.O. Box 101, 5900 MA Venlo, the Netherlands; and is part of the research programme VIDI with project number 15698, which is (partly) financed by the Netherlands Organisation for Scientific Research (NWO). The material in this paper was partially presented at the 18th IFAC Symposium on System Identification, July 9-11, 2018, Stockholm, Sweden and at the IEEE 15th International Workshop on Advanced Motion Control, March 9-11, 2018, Tokyo, Japan.

Email addresses: l.l.g.blanken@tue.nl (Lennart Blanken), t.a.e.oomen@tue.nl (Tom Oomen).

model complexity.. In particular, a possibly infinite-dimensional model is identified that is restricted to a reproducing kernel Hilbert space (RKHS). The RKHS can be designed to possess desired model properties, including smoothness and stability [9,27]. Note that these developments have strongly focused on causal and stable systems, since these are desirable properties for many physical systems in, e.g., simulation and prediction. In sharp contrast, considering only causality and stability directly limits potential benefits for feedforward control.

The main contribution of this paper is a framework for non-causal kernel-based regression and the design of the associated kernels that enable identification of non-causal, inverse, models. Constraints on inverse models can be directly enforced, including model complexity, stability aspects, and the degree of preview, enabling the desired performance benefits for feedforward control. This may be a direct advantage compared to the indirect approach of identification of the forward model, followed by an inversion step [6,33]. Furthermore, the mean square error (MSE) of the inverse system estimate is minimized [9], [18, Ch. 4]. Suitable non-causal kernels are developed, including non-causal stable spline (SS) kernels and kernels based on orthonormal basis functions (OBFs) in $\mathcal{L}_2$. Existing causal kernels are recovered as special cases, including causal SS kernels [9,27], and kernels based on OBFs in $\mathcal{H}_2$ [8,11]. Examples confirm the potential of the proposed identification method for feedforward control. The present paper substantially extends preliminary results in [3,4], including expanded theoretical developments, proofs, and non-causal kernel designs.

Notation. All systems are discrete-time, single-input, single-output and linear time-invariant. Let $\mathbb{D}$ denote the open unit disc, i.e., $\{z \in \mathbb{C} : |z| < 1\}$, $\mathbb{T}$ the unit circle, i.e., $\{z \in \mathbb{C} : |z| = 1\}$, and $\mathbb{E} = \mathbb{C} \setminus (\mathbb{D} \cup \mathbb{T})$ the exterior of the unit circle. The space $\ell_p(\mathbb{Z})$, $1 \leq p \leq \infty$, consists of all sequences on $t \in \mathbb{Z}$ with finite norm $\|x\|_p = (\sum_{t\in\mathbb{Z}} |x(t)|^p)^{1/p}$. The set of functions square integrable on $\mathbb{T}$ is denoted $\mathcal{L}_2(\mathbb{T})$. $\mathcal{H}_2(\mathbb{D})$ denotes the set of functions square integrable on $\mathbb{T}$ and analytic in $\mathbb{E}$, and $\mathcal{H}_2^\perp(\mathbb{D}) = \mathcal{L}_2(\mathbb{T}) \setminus \mathcal{H}_2(\mathbb{D})$. It is emphasized that, in discrete time, proper functions are included in $\mathcal{L}_2(\mathbb{T})$. The space $\mathcal{H}_{2-}(\mathbb{D})$ denotes all functions in $\mathcal{H}_2(\mathbb{D})$ that are zero at infinity, such as strictly causal systems. Let $P(z)$ denote a transfer function, q is the forward time-shift operator, i.e., $qx(t) = x(t+1)$, and $P(q)$ denotes the pulse-transfer operator associated with $P(z)$. Signals are often tacitly assumed of length N.

2 Problem formulation

In this section, the identification problem is defined. First, the role of inverse models for feedforward is clarified. Second, identification approaches for inverse models are investigated.

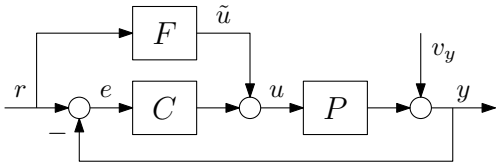

Fig. 1. Control configuration for inverse-model based feedforward: high tracking performance $e(t) = -Sv_y(t)$, i.e., elimination of the contribution of r, is achieved by $F = P^{-1}$.

2.1 Feedforward control and the role of inverse models

The goal in feedforward control is to minimize tracking error $e = r - y$ by the design of feedforward controller F, see Figure 1. Here, P denotes an unknown plant, C is a stabilizing feedback controller, r denotes a known reference signal, u and y are the input and output of P, respectively, $\tilde{u}$ is the feedforward signal, and v_y is a disturbance. Given r, the tracking error is described by

$$e(t) = S(q)\left(1 - P(q)F(q)\right) r(t) - S(q)v_y(t), \qquad (1)$$

with $S(q) = \frac{1}{1+P(q)C(q)}$. Optimal tracking performance in the sense of $e(t) = -Sv_y(t)$, i.e., elimination of the reference-induced contribution, is achieved by $F(q) = P^{-1}(q)$. Hence, feedforward control requires models of the inverse system. This examples provides a direction motivation to estimate inverse models $\widehat{P^{-1}}$ from data.

2.2 Identification of inverse models and regularization

The problem considered in this paper is the identification of P^{-1} from data $\{u(t), y(t)\}_{t=1}^N$. Two approaches can be distinguished. Essentially, these follow from a different choice of input and output, see also [10] for a fundamental motivation from a modeling perspective.

- A forward model $\hat{P}$ is estimated from input $u(t)$ and output $y(t)$, which is inverted to obtain $(\hat{P})^{-1}$, see, e.g., [6,33].
- An inverse model $\widehat{P^{-1}}$ is estimated directly from *input* $y(t)$ and *output* $u(t)$, see, e.g., [5,16,19].

Both approaches are equivalent if the number of data samples N tends to infinity. Asymptotically optimal estimates of P^{-1} are obtained by the maximum likelihood (ML) estimator, see, e.g., [16,21,30]. Under the assumption of additive i.i.d. noise on the output, both estimators of P^{-1} are consistent and achieve the Cramér-Rao lower bound. However, for small sample sizes, ML estimators may suffer from high variance, see, e.g., [26]. This directly relates to restricting the model order, e.g., using Akaike's information criterion or cross-validation [21,30], which poses a bias/variance trade-off.

Alternatively, kernel-based regularization methods aim to optimize the bias/variance trade-off through regular-

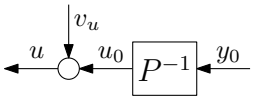

Fig. 2. Open-loop and backward system with noise-corrupted output. The aim is to estimate inverse model P^{-1} directly.

ization, see, e.g., [9,27]. The underlying model complexity is determined by a kernel, which can be exploited to impose prior knowledge as well as constraints. In view of this, the latter approach is preferred, i.e., to estimate $\widehat{P^{-1}}$ in the backward setting. The kernel enables to enforce desired properties of $\widehat{P^{-1}}$ in a direct manner, such as stability, smoothness, and finite preview/delay. In contrast, enforcing such desired properties through forward estimation of $\hat{P}$ and subsequent inversion may lead to substantial difficulties, since the inversion is often posed as an optimization problem, whose outcome depends on the model quality of $\hat{P}$ in a complex manner. The pursued approach is reminiscent to optimal input design, see, e.g., [17], where constraints on the inverse of the information matrix are directly enforced.

2.3 Problem formulation and contributions

Kernel-based regularized identification of P^{-1} is considered in the backward open-loop setting, illustrated in Figure 2. It is assumed that the measurement u of u_0 is contaminated with i.i.d. zero-mean normally distributed sequence $v_u(t)$ with variance $\sigma^2_{v_u}$, uncorrelated with y_0.

Example 1 *Examples of systems with noise-corrupted measurements of u_0 include vibration isolation systems, e.g., [28]. Measurements of input forces are typically noisy, whereas output position measurements are often reliable, e.g., using optical interferometers or encoders.*

If $P(z)$ has zeros in $\mathbb{E}$, i.e., NMP dynamics, then $P^{-1}(z)$ has poles outside the usual stability region $\mathbb{D}$. At present, such poles in $\mathbb{E}$ obstruct the successful use of kernel-based regularization techniques in inverse model identification, since existing results explicitly build upon stability, e.g., through stable spline kernels [27].

The main contribution of the paper is a kernel-based regularized identification approach for inverse systems, enabled by new kernel designs that enforce stability and non-causality. Subcontributions of the paper include:

- Non-causality is exploited to deal with unstable inverse systems (Subsection 3.1);
- Kernel-based regularization is generalized towards non-causal systems (Subsection 3.2), a range of the required non-causal kernels is provided (Section 4), and the overall procedure is summarized (Section 5);
- The benefits for feedforward control are demonstrated through simulations (Section 6).

3 A kernel-based regularization approach for non-causal systems

In this section, a kernel-based regularized approach is developed to estimate inverse models with poles in $\mathbb{D}$ and $\mathbb{E}$. The approach generalizes kernel-based identification towards the non-causal case, and recovers results for causal systems as a special case, see e.g., [9,27].

3.1 A non-causal view on poles in $\mathbb{E}$

In system identification, systems with poles in $\mathbb{E}$ are often interpreted as unstable, i.e., with causal and unbounded impulse response, see, e.g., [21]. This viewpoint is restrictive in certain situations. As is argued in Section 2.1, in feedforward control non-causal filtering operations are commonly performed since information on the future trajectory of $r(t)$ may be available. Relevant examples can be found in, e.g., [2,31,32], and include trajectory planning in robotics and motion control systems in mechatronics, including pick-and-place machines and printers. The key idea is to view $P^{-1}(z)$ as a non-causal and bounded operator on $\ell_2(\mathbb{Z})$. This has the following implication for system inversion.

Theorem 1 *(Non-causal exact inversion for NMP systems) Let system $P(z)$ be given such that $P^{-1}(z) \in \mathcal{RL}_2(\mathbb{T})$. Then, there exists a non-causal sequence $\theta^o \in \ell_1(\mathbb{Z})$ such that, for any signal $r(t) \in \ell_2(\mathbb{Z})$, the signal*

$$u_0(t) = \sum_{\tau=-\infty}^{\infty} \theta^o_\tau r(t-\tau) \in \ell_2(\mathbb{Z}) \tag{2}$$

leads to exact inversion $y_0(t) = P(q)u_0(t) = r(t)$.

Proof. Any $P^{-1}(z) \in \mathcal{RL}_2(\mathbb{T})$ admits a bilateral Z-transform, defined by two-sided formal Laurent series

$$P^{-1}(z) = \sum_{\tau=-\infty}^{\infty} \theta^o_\tau z^{-\tau}, \tag{3}$$

which converges in an annulus that includes $\mathbb{T}$. Since $\mathcal{RL}_2(\mathbb{T}) = \mathcal{RL}_\infty(\mathbb{T})$, the associated impulse response $\theta^o = \{\theta^o_\tau\}_{\tau=-\infty}^{\infty}$ is an element of $\ell_1(\mathbb{Z})$ [7, Theorem 2.1.10]. This implies that $P^{-1}(z)$ is a non-causal and bounded operator on $\ell_p(\mathbb{Z})$, $1 \le p \le \infty$, such that $u_0(t)$ in (2) is an element of $\ell_2(\mathbb{Z})$ for any $r(t) \in \ell_2(\mathbb{Z})$. Hence, $y_0(t) = \mathcal{Z}^{-1}\{P(z)P^{-1}(z)R(z)\} = \mathcal{Z}^{-1}\{R(z)\} = r(t)$, where $R(z)$ is the Z-transform of $r(t)$.

In view of Subsection 2.1, Theorem 1 states that optimal feedforward can be achieved for systems $P(z)$ with zeros in $\mathbb{E}$ through bounded inputs $\tilde{u}(t)$. The corresponding exact inverse $F(z) = P^{-1}(z)$ is non-causal.

Note that computing the exact inverse input (2) requires knowledge of the entire future trajectory $r(t)$, which may not be available. In practice often finite preview-based inputs are employed, see, e.g., [33], using the future trajectory within a preview time T_{pre} as

$$u_{0,\text{pre}}(t) = \sum_{\tau=-T_{\text{pre}}}^{\infty} \theta_\tau^o r(t-\tau). \tag{4}$$

The error between the exact inverse input $u_0(t)$ in (2) and finite-preview input $u_{0,\text{pre}}(t)$ can be made arbitrarily small by increasing T_{pre}, see [23,32]. The preview time T_{pre} required to guarantee a certain error depends on the smallest distance of the unstable poles of $P^{-1}(z)$ from $\mathbb{T}$.

Next, a kernel-based regularization approach for identification of non-causal systems is presented, and it is shown that causal systems are recovered as a special case.

3.2 Kernel-based regularization for non-causal systems

In view of Theorem 1, the aim is to restrict the estimate of θ^o to a reproducing kernel Hilbert space (RKHS) $\mathcal{H}$ that is a subset of $\ell_1(\mathbb{Z})$. In contrast, [9,26,27] consider causal systems with associated responses $\theta^0 \in \ell_1(\mathbb{N})$. Notice that $\ell_1(\mathbb{N}) \subset \ell_1(\mathbb{Z})$. Motivated by the results in Theorem 1, in the remainder we tacitly consider, possibly finite-order, impulse response models.

To allow for non-causality, the kernel-based regularized estimate is defined as

$$\hat{\theta} = \arg\min_{\theta\in\mathcal{H}} \sum_{t=1}^{N} \left(u(t) - \sum_{\tau=-\infty}^{\infty} \theta_\tau y_0(t-\tau) \right)^2 + \gamma \|\theta\|_{\mathcal{H}}^2, \tag{5}$$

where regularizer $\|\theta\|_{\mathcal{H}}^2$ is the squared induced norm on $\mathcal{H}$, and parameter $\gamma > 0$ weighs $\|\theta\|_{\mathcal{H}}^2$ with respect to the data fit. Note that (5) recovers the results from [26] if specific kernels are selected, see Section 4. The RKHS $\mathcal{H}$ is uniquely defined by a positive semidefinite kernel k, see [29, Definition 2.5], and is hence denoted $\mathcal{H}_k$ in the remainder. Minimizer $\hat{\theta}$ of infinite-dimensional problem (5) admits a finite-dimensional representation by the representer theorem, see, e.g., [26, Theorem 3], which can be directly generalized to allow non-causality by accommodating the two-sided series from (5).

The kernel can be designed to encode desired properties, including non-causality and boundedness of the inverse model in view of Theorem 1, represented by $\hat{\theta} \in \ell_1(\mathbb{Z})$. Existing kernels in literature often enforce $\hat{\theta} \in \ell_1(\mathbb{N})$, i.e., causal sequences, and are too restrictive in this sense.

4 Kernel design for non-causal systems

The aim of this section is to provide a range of suitable kernel structures for identification of inverse models with poles in $\mathbb{D}$ and $\mathbb{E}$. In view of Theorem 1, a key requirement on the kernels is that $\mathcal{H}_k \subset \ell_1(\mathbb{Z})$, which is implied by $k \in \ell_1(\mathbb{Z}^2)$. A proof follows from [12, Lemma 3], which is appropriately extended to the non-causal case. Indeed, non-causal kernels are defined to take inputs in $\mathbb{Z}^2$, in contrast with causal kernels that only take inputs in the subset $\mathbb{N}^2$. Note that anti-causal kernels take inputs in $\mathbb{Z}_-^2$, with $\mathbb{Z}_-$ the set of negative integers.

Next, kernel structures that satisfy $k \in \ell_1(\mathbb{Z}^2)$ are developed based on splines and orthonormal basis functions in $\mathcal{RL}_2(\mathbb{T})$. Tuning of the kernel parameters, called hyperparameters, can be performed using, e.g., marginal likelihood optimization with respect to data [26, Section 4.4]. Finally, priors and constraints that can be additionally included in non-causal kernels are investigated, including finite delay and preview as in, e.g., (4).

4.1 Non-causal stable spline kernels

Non-causal generalizations of stable spline kernels are developed, see, e.g., [27] for the causal case. The kernels enforce smoothness of $\hat{\theta}$ in (5), and exponential decay towards $t = \pm\infty$ in agreement with Theorem 1. Let

$$b(t) = \begin{cases} \lambda_{nc}^{-t} & \text{if } t < 0 \\ \lambda_c^t & \text{if } t \geq 0 \end{cases} \tag{6}$$

with $0 \leq \lambda_c, \lambda_{nc} < 1$. The non-causal first-order stable spline, also known as tuned/correlated (TC), and non-causal second-order stable spline (SS) kernels are given:

$$k_{TC}(t,t') = \alpha \min(b(t), b(t')), \tag{7}$$

$$k_{SS}(t,t') = \alpha \frac{\min(b(t),b(t'))^2}{6} \cdot \left(3\max(b(t),b(t')) - \min(b(t),b(t'))\right). \tag{8}$$

where $\alpha \geq 0$ is a scaling factor. Hyperparameters λ_c, λ_{nc} express decay rates for $t \geq 0$ and $t < 0$, respectively, and correlation between impulse response coefficients.

Remark 1 *The causal TC and SS kernels, see [9,27], are recovered by setting $b(t) = 0$ for $t < 0$ in (6). Rewriting and using the equalities $2\max(t,t') = t + t' + |t - t'|$ and $2\min(t,t') = t + t' - |t - t'|$ yields*

$$k_{TC}(t,t') = \alpha\lambda_c^{\max(t,t')} = \alpha\lambda_c^{t+t'}\lambda_c^{|t-t'|} \qquad \text{if } t,t' \in \mathbb{N}, \tag{9}$$

$$k_{SS}(t,t') = \alpha\lambda_c^{3(t+t')}\left(\frac{1}{2}\lambda_c^{|t-t'|} - \frac{1}{6}\lambda_c^{3|t-t'|}\right) \quad \text{if } t,t' \in \mathbb{N}, \tag{10}$$

and zero otherwise, e.g., $k_{TC}(t,t') = 0$ if $t < 0$ or $t' < 0$.

4.2 Non-causal kernels from OBFs in $\mathcal{RL}_2$

If prior knowledge is available on poles of $P^{-1}(z) \in \mathcal{RL}_2(\mathbb{T})$, e.g., complex conjugated poles of resonant dynamics, this can be appropriately expressed through kernel structures based on non-causal orthonormal basis functions (OBFs) in $\mathcal{RL}_2(\mathbb{T})$, see, e.g., [2]. This is presented next. The non-causal aspect is in contrast with causal kernels based on OBFs [8,11], which are based on OBFs in $\mathcal{RH}_{2-}(\mathbb{D})$, see, e.g., [14,24].

The kernels from OBFs in $\mathcal{RL}_2(\mathbb{T})$ are constructed as

$$k_{OBF}(t,t') = \sum_{k=1}^{n_c} \varphi_{c,k}(t)\varphi_{c,k}^\top(t') + \sum_{k=1}^{n_{ac}} \varphi_{ac,k}(t)\varphi_{ac,k}^\top(t'), \tag{11}$$

where $\varphi_{c,k}(t) \in \ell_2(\mathbb{N})$ and $\varphi_{ac,k}(t) \in \ell_2(\mathbb{Z}_-)$, with $\mathbb{Z}_-$ the set of negative integers, are the inverse Z-transforms of the rational orthonormal functions

$$\psi_{c,k}(z) = \frac{\sqrt{1-|\xi_{c,k}|^2}}{z-\xi_{c,k}} \prod_{i=1}^{k-1} \frac{1-\overline{\xi_{c,i}}z}{z-\xi_{c,i}}, \tag{12}$$

$$\psi_{ac,k}(z) = \frac{\sqrt{1-|\xi_{ac,k}|^2}}{1-\overline{\xi_{ac,k}}z} \prod_{i=1}^{k-1} \frac{z-\xi_{ac,i}}{1-\overline{\xi_{ac,i}}z}. \tag{13}$$

The functions (12), (13) are defined by sets of poles $\xi_c = \{\xi_{c,k}\}_{k=1,2,\dots,n_c} \subset \mathbb{D}$ and $\xi_{ac} = \{\frac{1}{\xi_{ac,k}}\}_{k=1,2,\dots,n_{ac}} \subset \mathbb{E}$, respectively, which are the hyperparameters of kernel (11). The orthonormality is with respect to the standard inner product on $\mathcal{L}_2(\mathbb{T})$, i.e., $\frac{1}{2\pi}\oint_{\mathbb{T}} \psi_k(z)\psi_j^*(z)dz = \delta_{k,j}$. The set $\{\psi_{c,k}\} \subset \mathcal{H}_{2-}(\mathbb{D})$ forms the Takenaka-Malmquist functions, and consists of strictly causal functions. The set $\{\psi_{ac,k}\} \subset \mathcal{H}_{2-}^\perp(\mathbb{D})$ contains anti-causal functions and direct feedthrough terms, e.g., select $\xi_{ac,0} = 0$ such that $\psi_{ac,0} = 1$. When complex conjugated pole pairs are used, (12) and (13) must be adapted through unitary transformations to obtain real-valued responses, see, e.g., [24] for a procedure.

For $\psi_{c,k}(z), \psi_{ac,k}(z) \in \mathcal{RL}_2(\mathbb{T}) = \mathcal{RL}_\infty(\mathbb{T})$, see [7, Theorem 2.1.10], and $\mathcal{H}_{k_{OBF}} = \text{span}(\varphi_c, \varphi_{ac})$, see [8,11], it follows that $\mathcal{H}_{k_{OBF}} \subset \ell_1(\mathbb{Z})$.

4.3 Additional priors and constraints on non-causality

The generalization of kernels to the non-causal case in Subsections 4.1 and 4.2 allows to embed additional priors and constraints on non-causal models. In particular:

- Finite preview and delay of inverse models can be directly enforced through truncations of non-causal kernels. This is often desired in, e.g., feedforward control [33]. As is argued in Subsection 3.1, the degree of preview and delay influences the inverse model accuracy, and consequently also feedforward control performance [33]. Their values can be interpreted as kernel hyperparameters and tuned from data [26, Section 4.4], or selected based on prior knowledge. For example, setting $k(t,t') = 0$ for all $|t| > T$ and $|t'| > T$ results in $\hat{\theta}_\tau = 0$ for $|\tau| > T$ in (5). Hence, the inverse model is described by $\widehat{P^{-1}}(z) = \sum_{\tau=-T}^{T} \hat{\theta}_\tau z^{-\tau}$.
- Zero correlation between causal ($t \geq 0$) and anti-causal ($t < 0$) elements can be expressed by setting $k(t,t') = 0$ for $t \geq 0, t' < 0$ and $t < 0, t' \geq 0$.

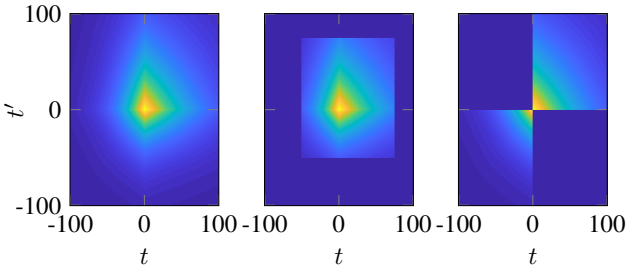

Fig. 3. Examples of modified non-causal stable spline kernels (8): full non-causal (left); truncated for finite preview and delay (middle); zero correlation between causal ($t, t' \geq 0$) and anti-causal ($t, t' < 0$) elements (right).

In view of the latter aspect, note kernels (7) and (8) express positive correlation between causal and anti-causal elements. This is not necessarily justified in view of the system $P^{-1}(z)$ to be identified, see (3), and is hence considered a design choice. To see this, let $P^{-1}(z) = [P^{-1}]_-(z) + [P^{-1}]_+(z)$, with $[P^{-1}]_-(z) \in \mathcal{RH}_2^\perp(\mathbb{T})$ and $[P^{-1}]_+(z) \in \mathcal{RH}_2(\mathbb{T})$, given by

$$[P^{-1}]_-(z) = \sum_{\tau=-\infty}^{-1} \theta_\tau^o z^{-\tau}, \quad [P^{-1}]_+(z) = \sum_{\tau=0}^{\infty} \theta_\tau^o z^{-\tau}. \tag{14}$$

Whether sequences $\{\theta_\tau\}_{\tau=-\infty}^{-1}$ and $\{\theta_\tau\}_{\tau=0}^{\infty}$ are correlated depends on the considered system. For example, mechanical structures may have pairs of zeros in $\mathbb{D}$ and $\mathbb{E}$ that are mirrored on the unit circle, see, e.g., [28, Chapter 6]. In contrast, for general $P^{-1}(z)$, systems $[P^{-1}]_-$ and $[P^{-1}]_+$ may be defined by independent sets of poles.

Example 2 *Examples of non-causal SS kernels* (8) *are depicted in Figure 3, including a truncated kernel for finite preview/delay, and a kernel that expresses zero correlation between causal and anti-causal elements.*

Remark 2 *The presented modifications to non-causal kernels preserve positive semidefiniteness (p.s.d.). Note that a kernel is p.s.d. if and only if all principal minors of the associated kernel matrices are nonnegative. That is, given a p.s.d. kernel, all square blocks centered on its main diagonal $t = t'$ are p.s.d. The considered modifications preserve such blocks, see Figure 3 for examples.*

5 Identification procedure

In previous Sections 3 and 4, a kernel-based identification approach for non-causal models is presented, and a range of non-causal kernels is provided. The presented framework is summarized in the following procedure.

Procedure 1 *(Kernel-based identification of inverse models) Given data* $\{y_0(t), u(t)\}_{t=1}^N$*, perform the following sequence of steps.*

(1) Select a suitable kernel structure, e.g., TC (7)*, SS* (8)*, or OBF* (11)*, where the following aspects are relevant in view of non-causality:*
- *a causal kernel, i.e.,* $k(t,t') = 0$ *for* $t, t' < 0$*, anti-causal kernel, i.e.,* $k(t,t') = 0$ *for* $t, t' \geq 0$*, or non-causal;*
- *if desired, set the correlation between causal and anti-causal elements in the kernel to zero, see Subsection 4.3.*
- *if desired, truncate the kernel for finite preview or delay, see Subsection 4.3.*

(2) Select the hyperparameters, e.g. by marginal likelihood optimization, see [26, Section 4.4], or based on prior knowledge.

(3) Given the designed kernel k*, compute minimizer* $\hat{\theta}$ (5) *and construct inverse model* $\widehat{P^{-1}}(z, \hat{\theta})$*.*

Remark 3 *For non-causal finite impulse response (FIR) models, i.e., truncations of* (3) *with* $\theta = [\theta_{-n_{ac}}, \ldots, \theta_{n_c}] \in \mathbb{R}^{n_\theta}$*,* $n_\theta = n_{ac} + 1 + n_c$*, problem* (5) *is equivalent to regularized least-squares [26, Section 11.3]:*

$$\hat{\theta} = \arg\min_{\theta} \|u_N - \Phi_N \theta\|_2^2 + \gamma \|\theta\|_{\mathcal{H}_K}^2 \tag{15}$$

$$= K\Phi_N^\top \left(\Phi_N K \Phi_N^\top + \gamma I_N\right)^{-1} u_N, \tag{16}$$

with $u_N \in \mathbb{R}^N$*, regression matrix* Φ_N *formed as* $\sum_{\tau=-\infty}^{\infty} \theta_\tau y_0(t_i - \tau) = \Phi_N(t_i, \cdot)\theta$ *with* $\Phi_N(t_i, \cdot)$ *the* i*th row of* Φ_N*, and matrix* $K \in \mathbb{R}^{n_\theta \times n_\theta}$ *with* $K_{ij} = k(t_i, t_j')$*.*

6 Example and application to feedforward

Next, Procedure 1 is applied in a simulation, and its benefits for feedforward control are demonstrated.

The considered data-generating system is described by $u(t) = P^{-1}(q)y_0(t) + v_u(t)$, see Figure 2, with true system

$$P(z) = \frac{1.550(z^2 - 2.035z + 1.052)(z^2 - 1.844z + 0.9391)}{z^2(z - 0.9514)(z - 0.9511)}. \tag{17}$$

The inverse $P^{-1}(z)$ has two unstable poles at $1.018 \pm 0.126i \in \mathbb{E}$, and two stable poles at $0.922 \pm 0.298i \in \mathbb{D}$.

Next, 1000 data sets $\{y_0(t), u(t)\}_{t=1}^N$ are generated. For each data set, the following two steps are performed:

(1) Identification of $\widehat{P^{-1}}$ according to Procedure 1, using data collected in the open-loop backward setting of Figure 2. The *input* $y_0(t)$ and *output* disturbance $v_u(t)$ are uncorrelated i.i.d zero-mean normally distributed noise sequences of length $N = 1000$, with variances $\sigma_{y_0}^2 = 1$, $\sigma_{v_u}^2 = 4$, respectively. The resulting signal-to-noise ratio on u is 11 dB.

(2) Application to feedforward: feedforward controller $F = \widehat{P^{-1}}$ from step 1) is implemented in the closed-loop control configuration of Figure 1, with feedback controller $C(z) = \frac{0.4102(z+1)}{z-0.7265}$. In this step, the *input* reference signal $r(t)$ is an i.i.d zero mean normally distributed noise sequence of length $N = 1000$ with variance $\sigma_r^2 = 1$, and $v_y(t) = 0$ to compare results based on disturbances from step 1) only. The norm $\|e\|_2$ of the tracking error $e = r - y$ is used to measure feedforward control performance.

6.1 Compared identification approaches

Non-causal FIR models are estimated with $n_{ac} = 300$ anti-causal terms and $n_c = 300$ causal terms, i.e., $\widehat{P^{-1}}(z) = \sum_{\tau=-300}^{300} \theta_\tau z^{-\tau}$. The use of the following kernels in step 1) of Procedure 1 is compared:

- $\mathcal{L}_2$-OBF kernel (11) with 2 poles in $\mathbb{D}$ and 2 poles in $\mathbb{E}$.
- $\mathcal{H}_2$-OBF kernel (11) with 4 poles in $\mathbb{D}$.
- Non-causal SS kernel (8) with and without correlation between positive and negative τ, see Subsection 4.3.
- Causal SS kernel (8), i.e., $b(t) = 0$ for $t < 0$.
- No regularization, i.e., $\gamma = 0$ in (5).

Results for the non-causal TC kernel (7) are omitted for brevity: it performs slightly worse than the non-causal SS kernel. The selection of hyperparameters in step 2) of Procedure 1, e.g., poles of OBF kernels and decay rates of SS kernels, is performed by marginal likelihood optimization with respect to the data [26, Section 4.4].

In addition, the above-listed approaches for direct identification of inverse models are compared to the traditional two-step approach of forward estimation of a low-order parametric model $\widehat{P}$, and subsequent inversion to obtain a non-causal inverse model $(\widehat{P})^{-1}$, see Section 2.2 and, e.g., [33]. The forward identification step utilizes an ARMAX model structure, which results from reformulating the backwards data-generating system $u(t) = P^{-1}(q)y_0(t) + v_u(t)$ to a forward setting. The ARMAX estimation is implemented using the Matlab System Identification Toolbox, with model orders corresponding to true system $P(z)$. Further details on the employed approach are provided in Appendix A.

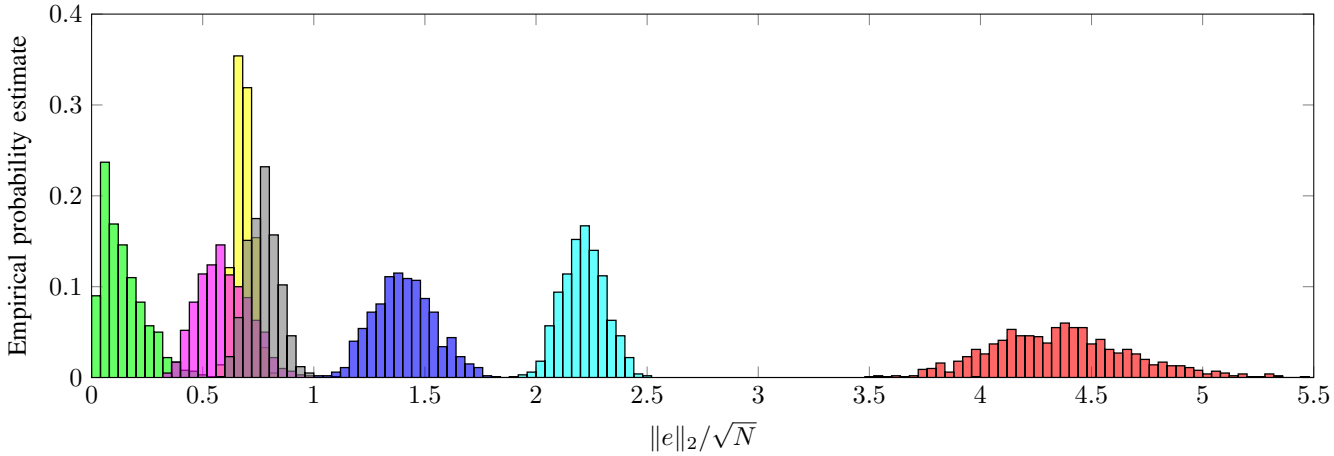

Fig. 4. Results of simulations: histogram of empirical probability estimate of tracking error $\|e\|_2$, obtained with identified inverse models implemented as feedforward controller, i.e., $F = \widehat{P^{-1}}$, see Figure 1. Not using regularization leads to poor performance (▮). The smallest error is obtained using the developed non-causal $\mathcal{L}_2$-OBF kernel (▮), whereas the use of a pre-existing causal $\mathcal{H}_2$-OBF kernel (▮) limits performance. Similar results hold for the developed non-causal stable spline kernel (▮) with respect to the causal stable spline kernel (▮). Removing the correlation between causal and anti-causal elements (▮) slightly increases performance. The traditional two-step approach of first estimating a low-order parametric forward model $\hat{P}$ and subsequent inversion to obtain $F = (\hat{P})^{-1}$ (▮) yields slightly worse performance than the kernel-based approaches with non-causal kernels.

6.2 Results: identified models and feedforward performance

The distribution of feedforward performance $\|e\|_2$ over the 1000 data sets is depicted in Figure 4, and estimates $\hat{\theta}$ from a single realization are shown in Figure 5 for each kernel design. The following observations are made:

- The non-causal $\mathcal{L}_2$-OBF kernel (green) outperforms all others in terms of tracking error, conforming its potential benefits for systems with dominant resonant dynamics. The estimate $\hat{\theta}$ closely approximates θ^o, see Figure 5. It is noted that the number of basis functions $n_c + n_{ac}$ in (11) equals the true system order: accurate system knowledge is employed.
- The non-causal SS kernel (magenta) leads to good performance, while requiring less detailed prior knowledge, e.g., the system order. The estimate $\hat{\theta}$ is smooth, see the inset in Figure 5, yet fails to accurately model the resonant dynamics. Including correlation between causal and anti-causal elements (yellow) does not lead to significant differences for this particular example system.
- All causal kernels, e.g., $\mathcal{H}_2$-OBF kernel (blue) and causal SS kernel (cyan), perform poorly. Indeed, causal kernels correspond to a causal RKHS, and hence enforce $\hat{\theta}_\tau = 0$ for $\tau < 0$. This can be observed in Figure 5, and leads to deteriorated performance in Figure 4.
- No regularization (red) leads to high variance of $\hat{\theta}$, resulting in poor performance, see Figure 4.
- The traditional two-step approach of forward identification (using a low-order ARMAX model) and subsequent inversion (gray) leads to worse performance than the proposed kernel-based approaches with non-causal kernels (green, magenta, yellow). This confirms benefits of kernel-based approaches compared to conventional prediction error methods, when dealing with noisy data records.

7 Conclusions

The presented kernel-based regularization framework enables accurate identification of non-causal models of inverse systems. The approach allows to enforce desired properties on the inverse models in a direct manner, including model complexity, and non-causality to deal with unstable systems. A range of the required non-causal kernels is developed, including generalizations of causal stable spline kernels and kernels based on orthonormal basis functions. The benefits of the developed framework for feedforward control performance are demonstrated through numerical simulations, including improvements compared to pre-existing causal kernels.

Acknowledgements

The authors would like to thank Ids van den Meijdenberg for his contributions to early stages of this work.

A Traditional two-step approach: forward identification and subsequent inversion

Details are presented on the traditional indirect approach for constructing inverse models, that is used in

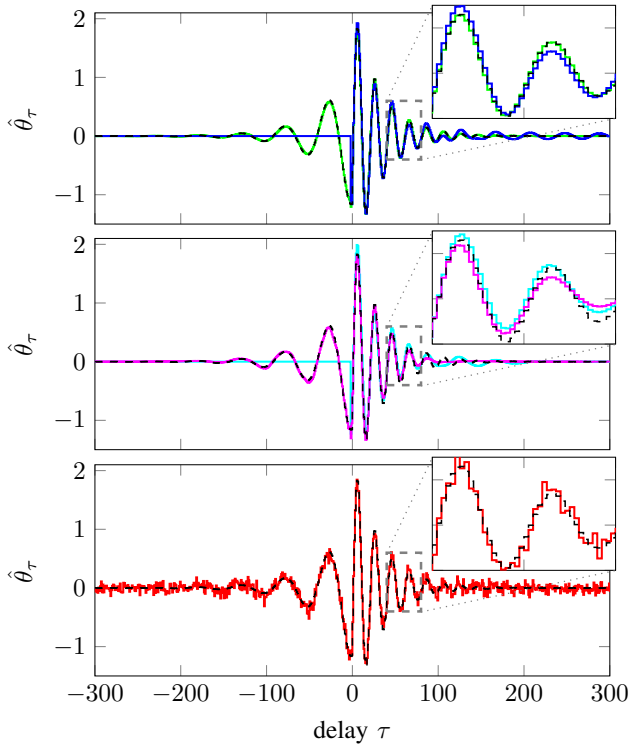

Fig. 5. Estimates $\hat{\theta}$ of models $\widehat{P^{-1}}(z) = \sum_{\tau=-300}^{300} \theta_\tau z^{-\tau}$ from single data realization, and true impulse response θ^o (- - -). The estimates using $\mathcal{L}_2$-OBF kernel (top, —), $\mathcal{H}_2$-OBF kernel (top, —), non-causal SS kernel (middle, —), causal SS kernel (middle, —), and estimate without regularization (bottom, —) confirm that i) kernel-based regularization enforces smoothness, ii) non-causal kernels are crucial to enable non-causal estimates, and iii) not using regularization leads to high variance.

Section 6 to compare with the developed direct method for identification of inverse models.

In view of the additive output noise assumption, note that the backward system configuration in Figure 2 can equivalently be interpreted in a forward configuration with output noise. This follows from a different choice of input and output, see also [10], and is illustrated in Figure A.1. The output disturbance v_u in the backward setting relates to the output disturbance in the forward setting through $v_y = -Pv_u$. An ARMAX model structure follows as a result of this noise coloring. In this paper, the forward model estimation is implemented using `armax.m` from the Matlab System Identification Toolbox, with model orders equal to the true system orders. The subsequent model inversion is performed according to Theorem 1.

References

[1] L. Blanken, F. Boeren, D. Bruijnen, and T. Oomen. Batch-to-batch rational feedforward control: from iterative learning to identification approaches, with application to a wafer stage. *IEEE/ASME Transactions on Mechatronics*, 22(2):826–837, 2017.

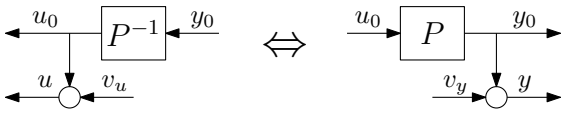

Fig. A.1. Backward and forward interpretations of open-loop system configuration. Equivalence holds if $v_y = -Pv_u$.

[2] L. Blanken, G. Isil, S. Koekebakker, and T. Oomen. Data-driven feedforward learning using non-causal rational basis functions: Application to an industrial flatbed printer. In *2018 IEEE American Control Conference*, pages 6672–6677, Milwaukee, WI, USA, 2018.

[3] L. Blanken, I. van den Meijdenberg, and T. Oomen. Inverse system estimation for feedforward: A kernel-based approach for non-causal systems. *IFAC-PapersOnLine*, 51(15):1050 – 1055, 2018. 18th IFAC Symposium on System Identification SYSID 2018.

[4] L. Blanken, I. van den Meijdenberg, and T. Oomen. Kernel-based regression of non-causal systems for inverse model feedforward estimation. In *2018 IEEE 15th International Workshop on Advanced Motion Control (AMC)*, pages 461–466, Tokyo, Japan, 2018.

[5] F. Boeren, T. Oomen, and M. Steinbuch. Iterative motion feedforward tuning: A data-driven approach based on instrumental variable identification. *Control Engineering Practice*, 37:11 – 19, 2015.

[6] J. Butterworth, L. Pao, and D. Abramovitch. Analysis and comparison of three discrete-time feedforward model-inverse control techniques for nonminimum-phase systems. *Mechatronics*, 22(5):577–587, 2012.

[7] J. Chen and G. Gu. *Control-oriented system identification: an H_∞ approach*. John Wiley & Sons, New York, NY, 2000.

[8] T. Chen and L. Ljung. Regularized system identification using orthonormal basis functions. In *Proceedings of the 2015 European Control Conference (ECC)*, pages 1291–1296, Linz, Austria, 2015.

[9] T. Chen, H. Ohlsson, and L. Ljung. On the estimation of transfer functions, regularizations and Gaussian processes-Revisited. *Automatica*, 48(8):1525 – 1535, 2012.

[10] A. Costalunga and A. Piazzi. A behavioral approach to inversion-based control. *Automatica*, 95:433–445, 2018.

[11] M. Darwish, G. Pillonetto, and R. Tóth. The quest for the right kernel in Bayesian impulse response identification: the use of OBFs. *Automatica*, 87:318 – 329, 2018.

[12] F. Dinuzzo. Kernels for linear time invariant system identification. *SIAM Journal on Control and Optimization*, 53(5):3299–3317, 2015.

[13] M. Gevers. A personal view of the development of system identification: A 30-year journey through an exciting field. *IEEE Control Systems Magazine*, 26(6):93–105, 2006.

[14] P. S. C. Heuberger, P. M. J. Van den Hof, and B. Wahlberg. *Modelling and Identification with rational orthogonal basis functions*. Springer-Verlag, London, UK, 2005.

[15] H. Hjalmarsson. From experiment design to closed-loop control. *Automatica*, 41(3):393 – 438, 2005.

[16] D. Ho and M. Enqvist. On the equivalence of forward and inverse IV estimators with application to quadcopter modeling. *IFAC-PapersOnLine*, 51(15):951–956, 2018. 18th IFAC Symposium on System Identification SYSID 2018.

[17] H. Jansson and H. Hjalmarsson. Input design via LMIs admitting frequency-wise model specifications in confidence regions. *IEEE Transactions on Automatic Control*, 50(10):1534–1549, Oct 2005.

[18] Y. Jung. *Inverse system identification with applications in predistortion*. PhD thesis, 2019. Linköping University.

[19] Y. Jung and M. Enqvist. Estimating models of inverse systems. In *Proceedings of the 52nd IEEE Conference on Decision and Control*, pages 7143–7148, Florence, Italy, 2013.

[20] J. Lataire and T. Chen. Transfer function and transient estimation by Gaussian process regression in the frequency domain. *Automatica*, 72:217 – 229, 2016.

[21] L. Ljung. *System identification - Theory for the User*. Prentice-Hall, Upper Saddle River, NY, USA, 1999.

[22] S. van der Meulen, R. Tousain, and O. Bosgra. Fixed structure feedforward controller design exploiting iterative trials: Application to a wafer stage and a desktop printer. *Journal of Dynamic Systems, Measurements, and Control*, 130(5):0510061–05100616, 2008.

[23] Richard H Middleton, Jie Chen, and James S Freudenberg. Tracking sensitivity and achievable $\mathcal{H}_\infty$ performance in preview control. *Automatica*, 40(8):1297–1306, 2004.

[24] B. Ninness and F. Gustafsson. A unifying construction of orthonormal bases for system identification. *IEEE Transactions on Automatic Control*, 42(4):515–521, 1997.

[25] T. Oomen and C. R. Rojas. Sparse iterative learning control with application to a wafer stage: Achieving performance, resource efficiency, and task flexibility. *Mechatronics*, 47:134 – 147, 2017.

[26] G. Pillonetto, F. Dinuzzo, T. Chen, G. De Nicolao, and L. Ljung. Kernel methods in system identification, machine learning and function estimation: A survey. *Automatica*, 50(3):657 – 682, 2014.

[27] G. Pillonetto and G. De Nicolao. A new kernel-based approach for linear system identification. *Automatica*, 46(1):81 – 93, 2010.

[28] A. Preumont. *Vibration control of active structures: an introduction*. Springer, 3 edition, 2011.

[29] B. Schölkopf and A. J. Smola. *Learning with kernels: support vector machines, regularization, optimization, and beyond*. The MIT Press, 2002.

[30] T. Söderström and P. Stoica. *System identification*. Prentice Hall, Hemel Hempstead, U.K., 1989.

[31] F. Song, Y. Liu, J. Xu, X. Yang, and Q. Zhu. Data-driven iterative feedforward tuning for a wafer stage: A high-order approach based on instrumental variables. *IEEE Transactions on Industrial Electronics*, 66(4):3106–3116, 2019.

[32] Q. Zou and S. Devasia. Preview-based stable-inversion for output tracking of linear systems. *Journal of Dynamic Systems, Measurements, and Control*, 121(4):625–630, 1999.

[33] J. van Zundert and T. Oomen. On inversion-based approaches for feedforward and ILC. *IFAC Mechatronics*, 50:282–291, 2018.